Available online at www.sciencedirect.com
ScienceDirect
Earth and Planetary Science Letters 260 (2007) 495–504
EPSL
www.elsevier.com/locate/epsl

Mantle plumes link magnetic superchrons to phanerozoic mass depletion events

Vincent Courtillot [a,*], Peter Olson [b]

[a] Institut de Physique du Globe de Paris, France
[b] Earth and Planetary Sciences, Johns Hopkins University, United States

Received 4 April 2007; received in revised form 21 May 2007; accepted 3 June 2007
Available online 12 June 2007
Editor: G.D. Price

Abstract

The four most recent large mass extinction events in the Phanerozoic – the Cretaceous–Tertiary (KT), the Triassic–Jurassic (TJ), and the Permo-Triassic (PT) and Guadalupian–Tatarian (GT) doublet – are associated with a major flood basalt eruption, with the timing of peak volcanic activity corresponding within measurement uncertainties to the extinction event. Three magnetic superchrons precede the four largest Phanerozoic extinctions. The Cretaceous Long Normal Superchron (duration ~35 Myr) precedes the KT and the Permian Kiaman Long Reversed Superchron (~50 Myr) precedes the PT–GT doublet. In addition, the newly recognized Ordovician Moyero Long Reversed Superchron (~30 Myr) precedes the end-Ordovician extinction event. There is a 10–20 Myr delay between the end of each superchron and the subsequent mass depletion event, both of which represent distant outliers from their respective populations. We propose that deep mantle plumes link these seemingly unrelated phenomena. Long-term (~200 Myr) variations in mantle convection possibly associated with the Wilson cycle induce temporal and spatial variations in heat flow at the core–mantle boundary. Polarity reversals are frequent when core heat flow is high and infrequent when it is low. Thermal instabilities in the D"-layer of the mantle increase core heat flow, end the magnetic superchron, and generate deep mantle plumes. The plumes ascend through the mantle on a 20 Myr time scale, producing continental flood basalt (trap) eruptions, rapid climatic change, and massive faunal depletions.

Keywords: magnetic superchrons; mantle plumes; faunal mass depletions; polarity reversals; continental flood basalts; traps; polarity reversals; geodynamo

1. Introduction

In a statistical and temporal reanalysis of Sepkoski's (1982) compilation of stratigraphic ranges for marine families of all animal taxa at the stage level, Bambach et al. (2004) showed that the "big five" mass extinctions recognized by most authors involve a decrease in genus diversity between 40% and 70%, and are actually better described as diversity depletion events. These include the end-Ordovician (440 Ma), the end-Guadalupian and end-Permian double event at 258 and 250 Ma, respectively, the end-Triassic (200 Ma) and the end-Cretaceous (65 Ma). They also showed that, although the Cambrian and early Ordovician (from 540 to 460 Ma) had an unusually large number of extinctions, they were different from these five major events and should not be included with them.

* Corresponding author.
E-mail address: courtil@ipgp.jussieu.fr (V. Courtillot).

0012-821X/$ - see front matter © 2007 Published by Elsevier B.V.
doi:10.1016/j.epsl.2007.06.003

Bambach et al. (2004) then asked the question whether the largest mass depletion events represent outliers compared to the entire extinction record and compared to shorter segments of geological time. Arranging the proportions of genus extinction in rank order by magnitude (see Fig. 1) they showed that two populations can be distinguished: a normal, background population of extinction magnitudes and a second one that includes the outliers, which are, in order of decreasing magnitude: the end-Permian (or end-Djhulfian), the end-Ordovician (or Late Ashgillian), the end-Guadalupian and the end-Cretaceous (or end-Maastrichtian), followed by the end Triassic (Late Norian). On the basis of their ranking, Bambach et al. (2004) concluded that "the five major mass depletions of diversity are so different in major features that it is clear they cannot have a common cause". In this paper, we point out that all these major mass depletion events are coeval with massive flood basalt eruptions, and follow in time by some 10 to 20 million years the ends of magnetic superchrons, unusually long periods when the geomagnetic field fails to reverse polarity. We propose that there is a causal link between these extreme events, involving changes in core–mantle boundary heat flow and generation of what we call "killer" mantle plumes.

2. Phanerozoic trap eruptions

Traps (or Continental Flood Basalts, CFBs, as they are also known) and ocean plateaus are the two primary types of Large Igneous Provinces (LIPs), massive outpourings of basaltic lavas that are not directly attributable to seafloor spreading processes (Mahoney and Coffin, 1997; Courtillot and Renne, 2003). At present there are about 15 known LIPS of Phanerozoic age (see Fig. 2). This may not be the full inventory, as some might have been erased by subduction, obscured by continental collision, or not yet identified. One example is the recently dated Emeishan Traps in China (~258 Ma), which were involved in the collision of India with Asia and the subsequent extrusion of Indochina, and have been severely diminished in surface outcrop area (see references in (Courtillot and Renne, 2003)).

It is possible that a substantial number of oceanic plateaus have been destroyed by subduction during this time or are as yet undetected, but this is not necessarily the case. If we limit consideration to the better-documented time since the beginning of the Mesozoic, there are 12 LIPs over 250 Myr, on average one per 20 Myr. Nine of these are in the interior or on the margin of continents (thus qualify as CFBs) and the other three are oceanic plateaus. The nine post-Paleozoic CFBs imply one such event every ~25 Myr on the continents, and given the mean age of the oceanic lithosphere (60 Ma, see (Cogné et al., 2006)), the most probable number of surviving oceanic plateaus is between 2 and 3. Accordingly, the current inventory of LIPs may be nearly complete (Courtillot et al., 2003), with the possible exception of the LIP that is expected to have initiated the Hawaiian hotspot track.

The correlation between mass extinctions, oceanic anoxia events (OAE) and other boundaries in the geological time scale with the dates of major trap eruptions was first pointed out by Rampino and Stothers (1988) and further documented by Courtillot (1994). This correlation has since been revised and updated several times, most recently by Courtillot and Renne (2003). As shown in Fig. 2, the four most recent of the big mass depletions (the end-Maastrichtian, end-Triassic, end-

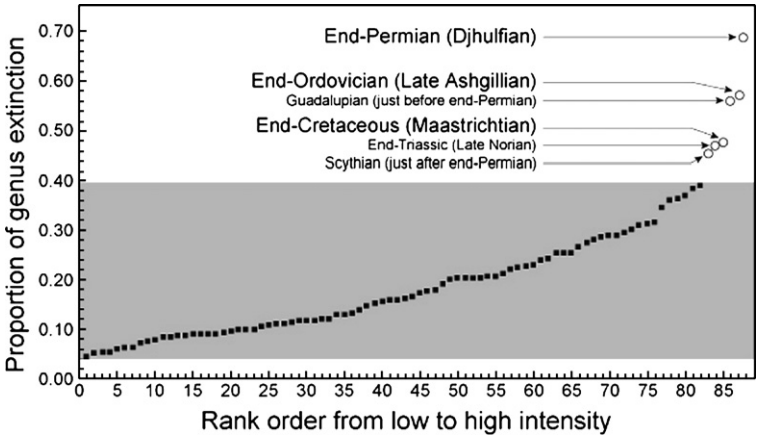

Fig. 1. Proportion of genus extinction arranged in rank order by magnitude (Middle Ordovician to Plio-Pleistocene values only) showing major Phanerozoic mass depletion events. After Bambach et al. (2004).

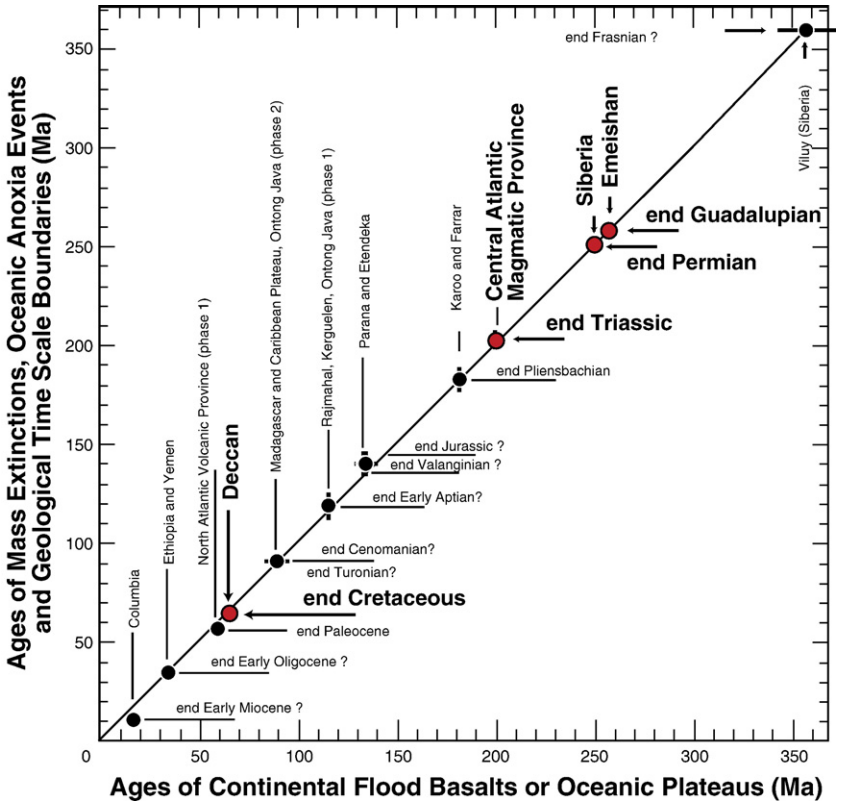

Fig. 2. Ages of the 15 major trap formation events in the Phanerozoic compared to mass extinction, paleoclimate events, and geological time scale boundaries. Red circles denote major mass depletions referred to in the text. After Courtillot and Renne (2003).

Permian, and end-Guadalupian, respectively) are each associated with a major trap (the Deccan traps, Central Atlantic Magmatic Province, Siberian traps, and Emeishan traps, respectively) with age of peak volcanism corresponding within experimental errors to extinction age. Traps associated with the end-Frasnian depletion event may have been recently found in the Viluy rift of Siberia (Kravchinsky et al., 2002), in which case only the end-Ordovician mass depletion event would be without a recognized trap.

All LIPs are associated with perturbations to the biosphere/atmosphere/hydrosphere system, although in many cases the amplitude of the perturbations may evidently be smaller than what is necessary for a major extinction event. For example, the 30 Ma Ethiopian and Yemen traps associate with the Oi2 early Oligocene climatic event, the 60 and 55 Ma North Atlantic Tertiary Province events associate with the end-Paleocene (a double pulse?), the 88 and 91 Ma Madagascar and Caribbean oceanic plateaus associate with the end-Cenomanian oceanic anoxia event and the end-Turonian extinction (another double pulse?), the Rajmahal traps and Kerguelen and Ontong–Java plateau events associate with the end-Early Aptian at ~110 Ma, the Parana and Etendeka traps associate with the end-Valanginian (not end-Jurassic) at ~133 Ma, and the Karoo and Farrar traps associate with the end-Pliensbachian at ~183 Ma. In contrast, the relatively small Columbia River Flood Basalt at ~15 Ma is not associated with any known global environmental perturbation. The record also includes evidence of the converse relationship, that traps are rare or missing during times without mass extinctions. For example, traps and significant extinction events are absent from the ~100 Myr interval between 258 and 360 Ma (Courtillot and Renne, 2003). In short, there is growing circumstantial evidence that major mass depletions, including the group identified by Bambach et al. (2004) and indeed all of the five major Phanerozoic faunal depletion events correlate in time with massive flood basalt eruptions.

3. Magnetic superchrons

For much of the past several hundred million years, the geodynamo has operated in a reversing state. Approximately 295 polarity reversals have been identified in the

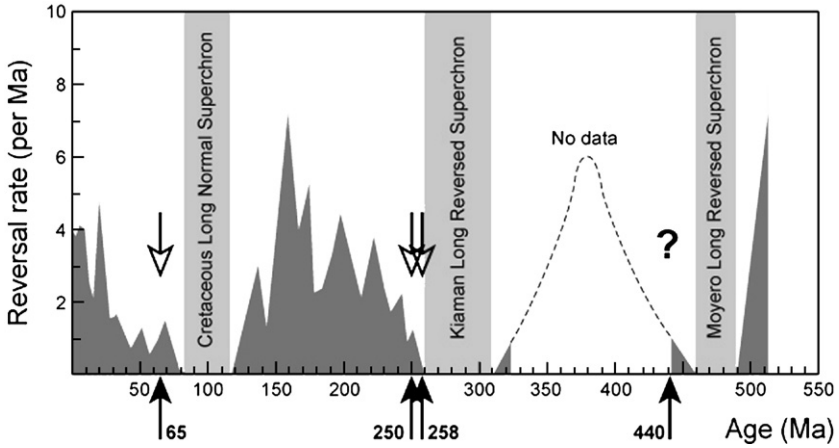

Fig. 3. Variation of geomagnetic polarity reversal frequency during Phanerozoic time compared with major faunal mass depletion events (up arrows) and associated trap eruptions (down arrows). Reversal rates are estimated according to Pavlov and Gallet (2005), by geological stage to harmonize pre- and post 150 Ma data, so that the overall, long-term envelope should be correct even if higher frequency details in post-150 Ma frequencies may not be quantitatively as accurate as oceanic anomalies and absolute dating of geological stages allows. Polarity superchrons are indicated by light shading.

158 Myr marine magnetic record (not including some 100 to 200 events called cryptochrons (Cande and Kent, 1992; Bouligand et al., 2006)), giving an average polarity reversal rate of just under two per million years. However, as Fig. 3 shows, the average reversal frequency has varied systematically through the Paleozoic, with three polarity superchrons, long intervals without reversals, separated by even longer time intervals when reversals were relatively frequent. Reversal frequency peaks about midway between successive superchrons and decreases prior to the superchron onset (Gallet et al., 1992; Opdyke and Channell, 1996).

The most recent superchron is the ~35 Myr long Cretaceous Long Normal Superchron (CLNS), which lasted from 118 to 83 Ma with normal (i.e., present-day) magnetic polarity. The ~50 Myr long Kiaman Long Reverse Superchron (KLNS) lasted from ~310 to ~260 Ma in the Carboniferous and Permian (Opdyke and Channell, 1996). The inventory of superchrons in the Phanerozoic has recently been augmented by acquisition of magnetostratigraphic data by Gallet and Pavlov (1996)), who found a third superchron in the Ordovician lasting ~30 Myr (from ~490 to ~460 Ma), which they have named the Moyero Long Reversed Superchron (MLRS) (Pavlov and Gallet, 2005). In aggregate the three superchrons span 20–25% of Paleozoic time.

4. The mantle plume connection

Shortly after evidence was put forward that the Deccan trap eruption had occurred at the KT boundary, Courtillot et al. (1986) and Courtillot and Besse (1987) pointed out that both events had occurred some 20 million years after the end of the CLNS. As discussed above, we now know of three magnetic superchrons in the Phanerozoic. In each instance the superchron ended several millions of years prior to one or two of the four major mass depletion events identified by Bambach et al. (2004), and in the case of the two most recent superchrons, prior to major trap eruptions. As shown in Fig. 3, the CLNS ends ~18 Myr prior to the eruption of the Deccan traps and the KLRS ends ~2–10 Myr prior to the Emeishan and Siberian trap doublet. The MLRS ends ~15–20 Myr prior to a mass extinction and a glaciation event at the end of the Ordovician, which we suggest were both due to the eruption of an as yet unrecognized trap (note that absolute ages for the onset and end of superchrons and mass extinctions are known to no better than 1–2% at most, implying potential uncertainties on the order of 5–10 Myr in the Paleozoic).

Is there a geophysical connection between traps and superchrons? There is broad consensus that traps originate from mantle plumes, either starting plumes (Courtillot et al., 2003) or plume surges (Mahoney and Coffin, 1997). Superchrons are usually attributed to time-variable thermal interaction between the core and the mantle, because the characteristic time scales of mantle convection processes (Schubert et al., 2001) are comparable to the 30–50 Myr duration and the ~200 Myr spacing of the superchrons, in contrast to the time scales of other geodynamo processes such as the convective overturn in the outer core, which are typically several orders of magnitude shorter (Hongre et al., 1998). Since the mantle controls the geodynamo by regulating the core–mantle boundary (CMB) heat flow (Labrosse, 2002; Roberts

et al., 2003), a natural way to end superchrons is by changing the heat flow at the CMB, as would occur during formation of thermal plumes in the D"-layer of the lower mantle (Olson, 2003).

The sensitivity of polarity reversal frequency to CMB heat flow variations is now only partially understood, and for a long time, even the "sign" of the effect was uncertain. Courtillot and Besse (1987) proposed that superchrons end through increased CMB heat flow, arguing that higher heat flow excites turbulent fluctuations in the core that produce polarity reversals. On the other hand, Larson and Olson (1991) proposed a relationship between the onset of the CLNS and the eruption of the Ontong–Java plateau based on kinematic dynamos that implied an inverse relationship between CMB heat flow and polarity reversal frequency. Gallet and Hulot (1997) proposed a scenario in which arrival of cold material (from a mantle avalanche (Machetel and Weber, 1991)) at the CMB, which could in turn trigger plume eruptions, perturb the geodynamo and initiate superchrons.

Recently, however, the connection between reversal frequency and thermal conditions at the CMB has become somewhat clearer. Self-consistent numerical dynamo models (Glatzmaier et al., 1999; Sarson and Jones, 1999; Kageyama et al., 1999; Kutzner and Christensen, 2002; Wicht and Olson, 2004; Takahashi et al., 2005) definitively show that the frequency of polarity reversals increases with the magnitude of CMB heat flow, and furthermore, that the reversal frequency is sensitive to the CMB heat flow pattern.

Fig. 4 shows qualitatively how the reversal frequency and the dipole moment depend on the average CMB heat flow, based on the systematics of a wide variety of convection-driven numerical dynamo models (Kutzner and Christensen, 2002; Christensen and Aubert, 2006; Olson and Christensen, 2006). In general, the sensitivity of reversal frequency to the average CMB heat flow depends on the proximity of the geodynamo to the transition from nonreversing to reversing dynamo states. If the geodynamo lies close to this transition, then increasing the average CMB heat flow by only a small amount, from q_1 to q_2 in Fig. 4 for example, would terminate a superchron. The same increase in average CMB heat flow would also slightly reduce the time-average dipole moment, according to Fig. 4.

Polarity reversal frequency is also sensitive to the pattern of heat flow on the CMB. Although not all aspects of this interaction have been investigated, numerical dynamo studies indicate that reversal frequency depends on whether the pattern of CMB heat flow matches or deviates from the intrinsic pattern of

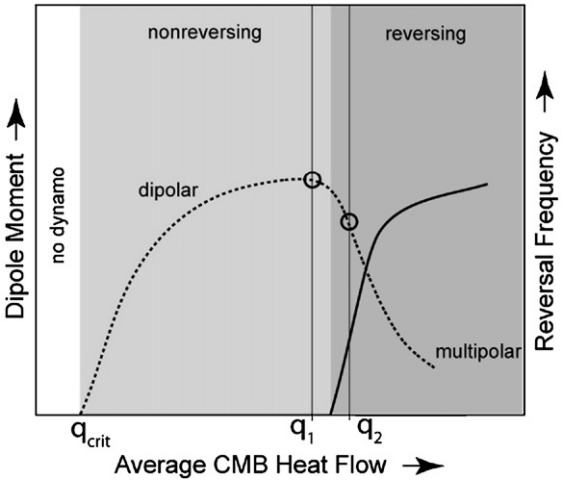

Fig. 4. Regime diagram showing the sensitivity of reversal frequency and dipole moment to the average core–mantle boundary (CMB) heat flow according to numerical dynamo models. Shading indicates subcritical (no dynamo), nonreversing (superchron), and reversing dynamo regimes, respectively. Solid curve is the variation in reversal frequency and dashed curve is the variation in dipole moment. CMB heat flows q_1 and q_2 correspond to superchron and reversing dynamo states, respectively.

convective heat transport in the outer core. The combination of strong rotational constraints and the core's spherical geometry dictates that convective heat transport in the outer core tends to be greatest in the equatorial region, with a secondary maximum near the poles in some cases (Glatzmaier and Roberts, 1995). Dynamo models that impose this pattern of heat flow on the CMB tend to produce strong, stable (non-reversing) axial dipole fields, whereas dynamo models that impose the opposite pattern tend to produce weaker dipole fields and more frequent reversals (Glatzmaier et al., 1999; Coe and Glatzmaier, 2006). We also note that numerical model results show that too much boundary heat flow heterogeneity generally cause dynamos to fail (Olson and Christensen, 2002).

Fig. 5 is a schematic illustration of the dynamo response to different patterns of CMB heat flow, according to the numerical model results. The horizontal coordinate is the average CMB heat flow, as in Fig. 4. The vertical coordinate in Fig. 5 is proportional to the amplitude of CMB heat flow heterogeneity q_{het}, with positive values representing those patterns that destabilize the geodynamo and negative values representing the same patterns but with the opposite sign. Suppose that the geodynamo occupies the superchron state labeled S in Fig. 5, in which the CMB heat flow has a relatively low average value q_1 and is spatially uniform. A thermal perturbation at the CMB resulting from formation of a

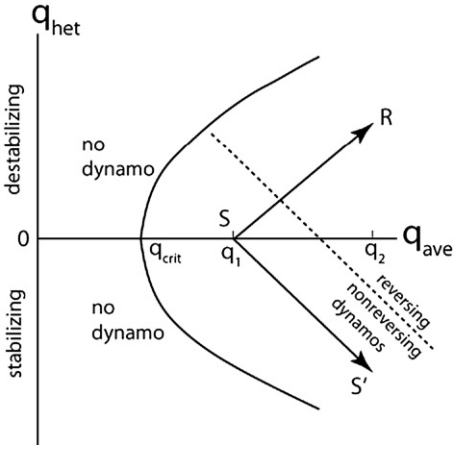

Fig. 5. Regime diagram showing dynamo sensitivity to core–mantle boundary (CMB) heat flow heterogeneity according to numerical models. q_{ave} denotes the average CMB heat flow, q_{het} is CMB heat flow heterogeneity. Negative q_{het} denotes heterogeneity patterns that increase dynamo polarity stability, positive q_{het} denotes heterogeneity patterns that decrease dynamo polarity stability. Dashed line marks transition from reversing to nonreversing dynamo states. Effects of two plume formation events are shown with arrows starting from superchron state S. Both events increase q_{ave}, but the perturbation leading to state *R* is destabilizing and ends the superchron, whereas the perturbation leading to S' does not.

plume in the D"-layer would increase the average CMB heat flow to q_2, and depending on where the plume forms, i.e. depending on the pattern of CMB heat flow heterogeneity it induces, would either increase or decrease superchron stability. For example, if the plume formation preferentially increases the equatorial heat flow, the geodynamo would move in the direction of point S' in Fig. 5. Such a change would not terminate the superchron. If instead the plume formation preferentially increases the mid-latitude heat flow, it would move the geodynamo in the direction of point R, thereby ending the superchron. Parallel considerations apply to the onset of a superchron. A thermal perturbation in the D"-layer that decreases both the average CMB heat flow and its heterogeneity can increase polarity stability and precipitate a superchron by moving the geodynamo generally downward and to the left in Fig. 5.

5. Superchrons and the Wilson cycle

We have argued for a link between trap eruptions and the end of magnetic superchrons in terms of mantle plume formation in the D"-layer. What controls the onset of the superchrons? The time intervals between superchrons are suggestive of the long-term variability in mantle dynamics that is loosely referred to as the Wilson cycle. Originally the Wilson cycle was used to describe episodes of continental collision and aggregation alternating with continental breakup and dispersal, but the concept has been extended to include long-term fluctuations in other Earth properties such as atmospheric CO_2 (Berner and Kothavala, 2001), global sea floor spreading rates (Cogné and Humler, 2004; Cogné et al., 2006; Conrad and Lithgow-Bertelloni, 2006), global sea level (Gaffin, 1987; Haq et al., 1987), polar motion (Courtillot and Besse, 1987), and tectonic and magmatic activity on the continents (Russo and Silver, 1996; Ryan and Dewey, 1997). Strictly speaking, many of these processes are not cyclical, and most of them (superchrons included) are poorly documented prior to the Phanerozoic. Even so, it is worthwhile determining if the Wilson cycle plays a role in the timing of superchrons, although we anticipate significant phase differences between events at the CMB and at the Earth's surface.

Fig. 6 illustrates some possible phase relationships between average surface heat flow and average CMB heat flow, derived from mantle convection models by Bunge et al. (2003) and Nakagawa and Tackley (2004a). The curve labeled "Slabs" denotes the CMB heat flow associated with a style of mantle convection driven by subduction and surface plate motions, with little or no contribution from buoyant plumes. As Fig. 6 indicates, this style of mantle convection is expected to produce CMB heat flow variations that are either in phase with or slightly lag the surface heat flow variations in time. Such

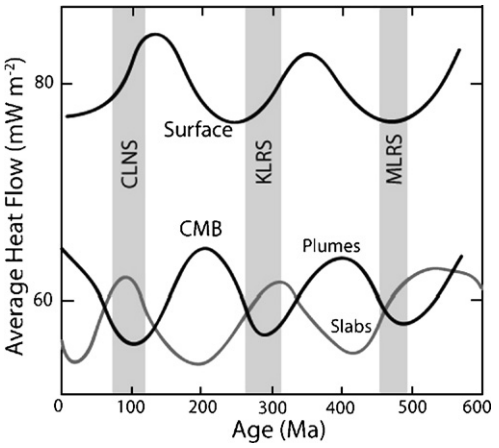

Fig. 6. Schematic of the time variation of average heat flow at the Earth's surface and at the core–mantle boundary (CMB) according to numerical models of whole mantle convection by Bunge et al. (2003) and Nakagawa and Tackley (2004a). The CMB heat flow variation in subduction-driven and plate-driven mantle convection (labeled Slabs) slightly lags the surface heat flow variation and magnetic superchrons (shaded bands) coincide with high CMB heat flow. In the alternative mantle convection model (labeled Plumes), the CMB heat flow variation is controlled by plume formation, leads the surface heat flow variation, and the magnetic superchrons coincide with low CMB heat flow.

models predict CMB heat flow maxima during the CLNS and KLRS times, and also predict low CMB heat flow at times when polarity reversals were frequent, both of which are at variance with the results of numerical dynamo models.

An alternative model is shown by the curve labeled "Plumes " in Fig. 6, in which CMB heat flow leads the surface heat flow by almost one-half cycle. This phase relationship assumes the CMB is heat flow controlled (at least in part) by mantle plume formation. Suppose that dense material accumulates in the D"-layer, during each major peak in mantle convective activity, temporarily stabilizing the D"-layer and reducing the heat flow from the core. Once CMB heat flow falls below a critical threshold, the geodynamo transitions to superchron state as illustrated in Fig. 4. The D"-layer then undergoes a transient phase of conductive growth, which continues until its thermal thickness becomes sufficiently large and its average viscosity sufficiently small to support boundary layer instabilities, which then grow into large mantle plumes. The end of each superchron corresponds to times when newly formed plumes alter the CMB heat flow regime in the manner depicted in Fig. 5. A substantial phase difference between heat flow at the surface and the CMB, in which the CMB generally leads the surface, would seem to demand that deep mantle plumes play a role in the heat transfer in the deep Earth that is somewhat independent of sea floor spreading and subduction processes.

6. Killer mantle plumes

Our hypothesis is that geomagnetic polarity superchrons ended by mantle plume formation, and after ascent through the mantle these plumes produced the trap eruptions that initiated Phanerozoic faunal mass depletion events. Jones et al. (2002) proposed a very different model, in which impacts initiate the trap eruptions. According to that model, the magnetic field response would come during or after the trap eruption (assuming the impact affected the geodynamo), in which case superchrons would postdate the events at the surface, contrary to the observed sequencing. The Jones et al. (2002) model is at variance with evidence from the Cretaceous–Tertiary boundary where impact-related products (iridium enriched sediments) overly the first volcanic flows in the Deccan traps (see discussion in (Courtillot and Renne, 2003)).

However, our model raises questions of its own. For example, only a fraction of the known Phanerozoic traps are timed to superchron and mass depletion events. What special properties would make this subset into killer mantle plumes? A number of attributes of flood basalt eruptions that could explain why two otherwise similar mantle plumes might have quite different impact on the biosphere or the climate system have been suggested (Courtillot and Renne, 2003). These include flood basalt volume, chemical composition (particularly sulfur), latitude of eruption, pre-existing state of the climate, and most importantly number, size and time signature of individual volcanic pulses that make up the event. The environmental impact must depend on the particulars of each event, including the paleogeography at the time of the eruption, the injection latitude, altitude, time history, and other parameters. Unfortunately, the response of the Earth system to these particulars is poorly known.

A related question is: which plume properties that affect the surface environment will also have a large effect on the core? One such property is plume rise time. The timing in Fig. 3 indicates about 10 Myr between the end of the superchron (when the core heat flow passes the superchron threshold) and the trap eruption and faunal mass depletion (when the plume reaches the lithosphere). This implies an average 0.3 m/yr plume ascent velocity through the mantle, which is about one order of magnitude higher than the average horizontal velocity associated with plate tectonics (Conrad and Lithgow-Bertelloni, 2006). Such high ascent velocities would require a massive buoyant head for a starting plume (Richards et al., 1989; White and McKenzie, 1995) or alternatively, a plume soliton traveling through a pre-existing mantle conduit (Schubert et al., 2001). The plume characteristics we infer (chemical heterogeneity and fast ascent) are similar to thermochemical instabilities: Le Bars and Davaille (2004) discuss such large trap-producing thermochemical heads, where chemical compositional differences involve Fe content. The short ascent time ensures that the plume material would loose very little of its excess potential temperature during ascent, would arrive at the lithosphere with abundant superheat, and would probably erupt over a short time interval.

Excess potential temperature and rapid ascent seem to be promising explanations for why only a small number of mantle plumes become killers, altering both the geodynamo (via CMB heat loss) and the surface environment (via eruption products), while the majority of plumes, including some apparently large ones, have weaker effects. Killer plumes might form especially close to the CMB, possibly in the seismic Ultra Low Velocity Zone (ULVZ; see (Garnero, 2000)) thereby inheriting higher than average excess temperature that could survive transport through the subadiabatic interior of the mantle

(Bunge, 2005). In light of the dynamical complexity in the D" region, including the post-perovskite mineralogy (Nakagawa and Tackley, 2004b), it is likely that plumes originating at different locations and sampling different material from different levels in D" will inherit different potential temperatures. Furthermore, if the killer plumes tap the ULVZ they could possibly incorporate a chemical signature that might be missing or reduced in other plumes that form further up in the lower mantle. Heavy sampling of the ULVZ would also be consistent with an elevated potential temperature in plumes formed there, as well as a large CMB heat flux pulse, resulting in a more direct effect on the geodynamo. It has been proposed that S is the key element of climate change and global poisoning (Self et al., 1997; Self et al., in press; Chenet et al., 2005; Chenet et al., in press). Since S and Fe are related (Fe content is used as a proxy to estimate how much S could be degassed by a given trap), the S and Fe content of the D"-layer might inversely correlate with distance from the CMB, being larger in the ULVZ than elsewhere.

Finally, we discuss some observations and numerical simulations that would help in testing some of the predictions of our model. One model prediction is that the transition from non-reversing to reversing dynamo states should be accompanied by a decrease in dipole moment and also a decrease in dipolarity. Recent assessments of the long-term trends in geomagnetic paleointensity (Tauxe, 2006; Tarduno, et al., 2006) seem to converge towards the original suggestion of Cox (1968) that there is a positive correlation between high field strength and low reversal frequency. In particular, Tarduno et al. (2006) conclude that the time-averaged field is stronger and more dipolar when it is in a superchron state, consistent with Fig. 4.

We have suggested that depending on where a plume forms, the resulting heat flow perturbation could either increase or decrease the geodynamo polarity stability. Plume formation in the equatorial or polar regions is less likely to terminate a superchron, compared with the same plume formed at middle latitude. Connections between CMB heat flow heterogeneity and the polarity stability of dynamo calculations have already been reported (Glatzmaier and Roberts, 1995; Glatzmaier et al., 1999; Coe and Glatzmaier, 2006) and could be quantified by systematic modeling. This relationship might also be testable using the distribution of trap paleolatitudes. The available data present a mixed picture in this regard. The Siberian traps were erupted at polar latitudes, the Ethiopian, Caribbean, CAMP and Emeishan traps at equatorial latitudes, and most of the remainder at middle latitudes (NATP, Deccan, Madagascar, Parana–Etendeka, Karoo; (see (Courtillot and Renne, 2003) and (Davaille et al., 2005) Fig. 4). Alternatively, we suggested that anomalous plume potential temperature might be the decisive factor. We note that this explanation can also be tested, since it is now possible to estimate the plume potential temperature anomaly from hotspot volcanics (Bourdon et al., 2006).

Finally, our use of radiometric age data in this paper highlights the need for improved time resolution of the geophysical events in the deep past (superchron timing and trap eruptions) and better time sequencing of genera numbers in the paleontological record. In the latter case, for example, Stanley and Yang's (1994) subdivision of the last stages of the Permian into sub-stages was key to show that a seemingly 10 Myr-long event was actually a set of two short (~1 Myr) pulses separated by a ~8 Myr-long quiescence period. Such high resolution is not available for most stages now, although it would be very useful, for instance, to resolve the five cases of double pulses we have mentioned. We clearly need to improve resolution to the sub-interval level if we wish to perform more meaningful statistical analyses.

Acknowledgements

We thank Yves Gallet, Jean Besse, Emmanuel Dormy, Anne Davaille and Jean-Jacques Jaeger for comments on this manuscript. This research has been supported by NSF grants EAR-0604974 and 0652568 and an Institut Universitaire de France (IUF) Senior Fellowship to VC. IPGP Contribution 2256.

References

Bambach, R.K., Knoll, A.H., Wang, S.C., 2004. Origination, extinction, and mass depletion on marine diversity. Paleobiology 30, 522–542.

Berner, R.A., Kothavala, Z., 2001. GEOCARB III: a revised model of atmospheric CO_2 over Phanerozoic time. Amer. J. Sci. 310, 182–204.

Bouligand, C., Dyment, J., Gallet, Y., Hulot, G., 2006. Geomagnetic field variations between chrons 33r and 19r (83–41 Ma) from sea-surface magnetic anomaly profiles. Earth Planet. Sci. Lett. 250, 541–560.

Bourdon, B., Ribe, N.M., Stracke, A., Saal, A.E., Turner, S.P., 2006. Insights into the dynamics of mantle plumes from uranium-series geochemistry. Nature 444, 713–717.

Bunge, H.P., 2005. Low plume excess temperature and high core heat flux inferred from non-adiabatic geotherms in internally heated mantle circulation models. Phys. Earth. Planet. Sci. Lett. 153, 3–10.

Bunge, H.P., Hagelberg, C.R., Travis, B.J., 2003. Mantle circulation models with variational data assimilation: inferring past mantle flow structures from plate motion histories and seismic tomography. Geophys. J. Int. 152, 280–301.

Cande, S., Kent, D., 1992. A new geomagnetic polarity time scale for the Late Cretaceous and Cenozoic. J. Geophys. Res. 97, 13917–13951.

Chenet, A.L., Fluteau, F., Courtillot, V., 2005. Massive pollution following the largest historical basaltic fissure eruption: modelling the climatic effects of the 1783–1784 Laki event. Earth Planet. Sci. Lett. 236, 721–731.

A.L. Chenet, F. Fluteau, V. Courtillot, M. Gérard, M., K.V. Subbarao, in press. Determination of rapid Deccan eruptions across the KTB using paleomagnetic secular variation: (I) Results from a 1200 m-thick section in the Mahabaleshwar escarpment, J. Geophys. Res.

Christensen, U.R., Aubert, J., 2006. Scaling properties of convection-driven dynamos in rotating spherical shells and application to planetary magnetic fields. Geophys. J. Int. 166, 97–114.

Coe, R.S., Glatzmaier, G.A., 2006. Symmetry and stability of the geomagnetic field. Geophys. Res. Lett. 33, L21311. doi:10.1029/2006GL027903.

Cogné, J.P., Humler, E., 2004. Temporal variations of oceanic spreading and crustal production rates during the last 180 My. Earth Planet. Sci. Lett. 227, 427–439.

Cogné, J.P., Humler, E., Courtillot, V., 2006. Mean age of oceanic lithosphere drives eustatic sea-level change since Pangea breakup. Earth Planet. Sci. Lett. 245, 115–122.

Conrad, C.P., Lithgow-Bertelloni, C., 2006. Faster seafloor spreading and lithospheric production during the mid-Cenozoic. Geology 35, 29–32.

Courtillot, V., 1994. Mass extinctions in the last 300 million years: one impact and seven flood basalts? Isr. J. Earth-Sci. 43, 255–266.

Courtillot, V., Besse, J., 1987. Magnetic field reversals, polar wander, and core–mantle coupling. Science 237, 1140–1147.

Courtillot, V., Renne, P., 2003. On the ages of flood basalt events. Comp. Rendus Geosci. 335, 113–140.

Courtillot, V., Besse, J., Vandamme, D., Montigny, R., Jaeger, J.J., Cappetta, H., 1986. Deccan flood basalts at the Cretaceous/Tertiary boundary? Earth Planet. Sci. Lett. 80, 361–374.

Courtillot, V., Davaille, A., Stock, J., Besse, J., 2003. Three distinct types of hotspots in the Earth's mantle. Earth Planet. Sci. Lett. 205, 285–308.

Cox, A.V., 1968. Lengths of geomagnetic polarity intervals. J. Geophys. Res. 73, 3247–3260.

Davaille, A., Stutzmann, E., Silveira, G., Besse, J., Courtillot, V., 2005. Convective patterns under the Indo-Atlantic box. Earth Planet. Sci. Lett. 239, 233–252.

Gaffin, S., 1987. Ridge volume dependence on sea floor generation rate and inversion using long-term sea level change. Am. J. Sci. 287, 596–611.

Garnero, E.J., 2000. Heterogeneity of the lowermost mantle. Annu. Rev. Earth Planet. Sci. 509–537.

Gallet, Y., Hulot, G., 1997. Stationary and nonstationary behaviour within the geomagnetic polarity time scale. Geophys. Res. Lett. 24, 1875–1878.

Gallet, Y., Pavlov, V., 1996. Magnetostratigraphy of the Moyero river section (north-western Siberia): constraints on geomagnetic reversal frequency during the early Paleozoic. Geophys. J. Int. 125, 95–105.

Gallet, Y., Besse, J., Krystyn, L., Marcoux, J., Théveniaut, H., 1992. Magnetostratigraphy of the Late Triassic Bolücektasi Tepe section (southwestern Turkey): implications for changes in magnetic reversal frequency. Phys. Earth Planet. Inter. 73, 85–108.

Glatzmaier, G.A., Roberts, P.H., 1995. A three-dimensional self-consistent computer simulation of a geomagnetic field reversal. Nature 377, 203–209.

Glatzmaier, G.A., Coe, R.S., Hongre, L., Roberts, P.H., 1999. The role of the Earth's mantle in controlling the frequency of geomagnetic reversals. Nature 401, 885–890.

Haq, B.U., Hardendol, J., Vail, P.R., 1987. Chronology of fluctuating sea levels since the Triassic. Science 235, 1156–1167.

Hongre, L., Hulot, G., Khokhlov, A., 1998. An analysis of the geomagnetic field over the past 2000 years. Phys. Earth Planet. Inter. 106, 311–335.

Jones, A.P., Price, G.D., Price, N.J., DiCarli, P.S., Clegg, R.A., 2002. Impact induced melting and the development of large igneous provinces. Earth Planet Sci Lett. 202, 551–561.

Kageyama, A., Ochi, M.M., Sato, T., 1999. Flip-flop transitions of the magnetic intensity and polarity reversals in the magnetohydrodynamic dynamo. Phys. Rev. Lett. 82, 5409–5412.

Kravchinsky, V.A., Konstantinov, K.M., Courtillot, V., Savrasov, J.I., Valet, J.P., Chernyi, S., Mishenin, S., Parasotka, B., 2002. Paleomagnetism of East Siberian Traps and kimberlites: two new poles and paleogeographic reconstructions at about 360 and 250 Ma. Geophys. J. Int. 148, 1–33.

Kutzner, C., Christensen, U., 2002. From stable dipolar to reversing numerical dynamos. Phys. Earth Planet. Inter. 121, 29–45.

Larson, R.L., Olson, P., 1991. Mantle plumes control magnetic reversal frequency. Earth Planet. Sci. Lett. 107, 437–447.

Labrosse, S., 2002. Hotspots, mantle plumes and core heat loss. Earth Planet Sci. Lett. 199, 147–156.

Le Bars, M., Davaille, A., 2004. Whole layer convection in an heterogeneous mantle. J. Geophys. Res. 109. doi:10.1029/2003JB002617.

Machetel, P., Weber, P., 1991. Intermittent layered convection in a model with an endothermic phase change at 670 km. Nature 350, 55–57.

Mahoney, J.J., Coffin, M.F. (Eds.), 1997. Large igneous provinces: continental, oceanic and, planetary flood volcanism. AGU Geophysical Monograph, 100.

Nakagawa, T., Tackley, P.J., 2004a. Effects of thermo-chemical convection on the thermal evolution of the Earth's core. Earth Planet. Sci. Lett. 220, 107–119.

Nakagawa, T., Tackley, P.J., 2004b. Effects of a perovskite–post perovskite phase change near core–mantle boundary in compressible mantle convection. Geophys. Res. Lett. 31 (16), L16611. doi:10.1029/2004GL020648.

Olson, P., 2003. Thermal interaction of the core and mantle. In: Jones, C.A., Soward, A.M., Zhang, K. (Eds.), Earth's Core and Lower Mantle. Taylor and Francis, London and New York. 218 pp.

Olson, P., Christensen, U.R., 2002. The time-averaged magnetic field in numerical dynamos with non-uniform boundary heat flow. Geophysical Journal International 151, 809–823.

Olson, P., Christensen, U.R., 2006. Dipole moment scaling for convection-driven planetary dynamos. Earth Planet. Sci. Lett. 250, 561–571.

Opdyke, N., Channell, J.E.T., 1996. Magnetic stratigraphy. Int. Geophys. Ser., vol. 64. Academic Press, San Diego. 346 pp.

Pavlov, V., Gallet, Y., 2005. A third superchron during the Early Paleozoic. Episodes 28, 1–7.

Rampino, M.R., Stothers, R.B., 1988. Flood basalt volcanism during the past 250 million years. Science 241, 663–668.

Richards, M., Duncan, R., Courtillot, V., 1989. Flood basalts and hotspot tracks: plume heads and tails. Science 246, 103–107.

Roberts, P.H., Jones, C.A., Calderwood, A., 2003. Energy fluxes and Ohmic dissipation in the Earth's core. In: Jones, C.A., Soward, A.M., Zhang, K. (Eds.), Earth's Core and Lower Mantle. Taylor and Francis, London and New York. 218 pp.

Russo, R.M., Silver, P.G., 1996. Cordillera formation, mantle dynamics and the Wilson cycle. Geology 24 (6), 511–514.

Ryan, P.D., Dewey, J.F., 1997. Continental eclogites and the Wilson Cycle. J. Geol. Soc. 154, 437–442.

Sarson, G.R., Jones, C.A., 1999. A convection driven geodynamo reversal model. Phys. Earth Planet. Inter. 111, 3–20.

Schubert, G., Turcotte, D.L., Olson, P., 2001. Mantle Convection in the Earth and Planets. Cambridge University Press, Cambridge. 940 pp.

Self, S., Thordarson, T., Keszthelyi, T., 1997. Emplacement of continental flood basalts lava flows. In: Mahoney, J.J., Coffin, M.F. (Eds.), Large igneous provinces: Continental, oceanic, and planetary flood volcanism. Geophys. Monogr., vol. 100, pp. 381–410.

S. Self, T. Thordarson, M. Widdowson, A. Jay, in press. Volatile fluxes during flood basalt eruptions and potential effects on the global environment: a Deccan perspective, Earth Planet. Sci. Lett.

Sepkoski, J.J., 1982. A compendium of fossil marine families. Milwaukee Public Museum Contributions to Biology and Geology, vol. 51.

Stanley, S.M., Yang, X., 1994. A double mass extinction at the end of the Paleozoic era. Science 266, 1340–1344.

Takahashi, F., Matsushima, M., Honkura, Y., 2005. Simulations of a quasi-Taylor state geomagnetic field including polarity reversals on the Earth Simulator. Science 309, 459–461.

Tarduno, J., Cottrell, R.D., Smirnov, A.V., 2006. The paleomagnetism of single silicate crystals: recording geomagnetic field strength during mixed polarity intervals, superchrons, and inner core growth. Rev. Geophys. 41, RG1002. doi:10.1029/2005RG000189.

Tauxe, L., 2006. Long-term trends in paleointensity: the contribution of DSDP/ODP submarine basaltic glass collections. Phys. Earth Planet. Inter. 156, 223–241.

White, R.S., McKenzie, D., 1995. Mantle plumes and flood basalts. J. Geophys. Res. 100, 17543–17585.

Wicht, J., Olson, P., 2004. A detailed study of the polarity reversal mechanism in a numerical dynamo model. Geochem. Geophys. Geosys. 5. doi:10.1029/2003GC000602.